Metallographic Techniques for the Determination of the Martensite Transformation Start Forming Temperature in Medium Carbon Vanadium Titanium and Titanium Free Micro Alloyed Steel

Abdulnaser H. Fadel[1]*, Nenad A. Radovic[2]

[1]Al Zawia University, Faculty of Natural Resources Engineering, Al Zawia - Libya

[2] Belgrade University, Faculty of Technology and Metallurgy

***E-mail: A.fadel@zu.edu.ly**

Abstract

The main goal of the current paper is focused to investigate and reveal the importance critical transition temperatures. Different techniques were used to reveal the critical transition temperatures. The medium carbon vanadium titanium and titanium free micro alloyed steels tested in this work by isothermal treatment. In order to reveal experimentally the critical forming temperatures and compare it by predicted using equations and also describe the influence of alloying elements (Titanium) on the transformation behavior, martensitic starting formation temperature. This study has been carried out over a wide range of isothermal treatment temperature (270-350 °C). Samples were investigated using optical microscope (OM) and Field Emission Gun Scanning Electron Microscopy (FEGSEM) and it has been found that the tested procedure method give excellent results for the medium carbon vanadium titanium and titanium free micro alloyed steels.

Keywords: Medium Carbon Vanadium Titanium and Titanium Free Micro Alloyed Steel, Field Emission Gun Scanning Microscope (FEGSEM), Martensite Start (Ms) Forming Temperature and Grain Boundary Ferrite.

1. Introduction

Martensite in steels is a supersaturated solid solution of carbon in ferritic iron. Two different morphologies are observed in ferrous martensite microstructures: plate martensite and lath martensite, as shown in Fig. 1 [1,2,4]. A characteristic of plate martensite is the zigzag pattern of smaller plates as shown in Fig.1 (b) and Fig. 2. (a) [5, 6], which is formed later in the transformation. Smaller planes are bounded by adjacent larger plates that were formed at the beginning of the transformation. An important feature of plate martensite is the presence of microcracks (Fig. 2 a). These cracks occur when adjacent martensite crystals impinge on each other. Due to the shear-type mechanism, the transformation velocity of martensite can approach 10^6 mm/s, and thus growing martensite plates can achieve a significant amount of momentum. Impacts between moving plates create these microcracks [4]. However, the substructure of plate martensite consists of transformation twins, as a result of the shear mechanism that occurred during the transformation. The, regions in between the martensite plates in these micrographs are leftover parent phase that did not transform to martensite, called retained austenite, (the region between these packets is retained austenite). Retained austenite between martensite plates is easily resolvable by the light optical microscope. The other major martensite morphology is lath martensite (Fig. 1 a) in some times, referred to as packet martensite. The structure of most hardened steels is lath martensite. Figure 3 (a) is a micrograph of lath martensite in Fe-0.2C alloy. The dashed lines trace out prior austenite grain boundaries and the dark regions labeled A, B, and C are martensite laths. The term lath refers to the fine structure of the martensite crystal i.e. lath martensite is much finer than plate martensite. As shown in Figure 3(b), laths tend to align themselves into groups with the same orientation; these groups are termed packets**.** With regard to a packet of martensite laths, the transmission electron microscopy (TEM) is usually used to show it. The substructure of lath martensite consists of a network of dislocations, a result of the shear processes during transformation. As with plate martensite, retained austenite can be present in lath martensite, both in

between packets and between individual laths. Due to the difference in martensite morphology scale, the quantity of retained austenite in lath martensite is significantly less than that for plate

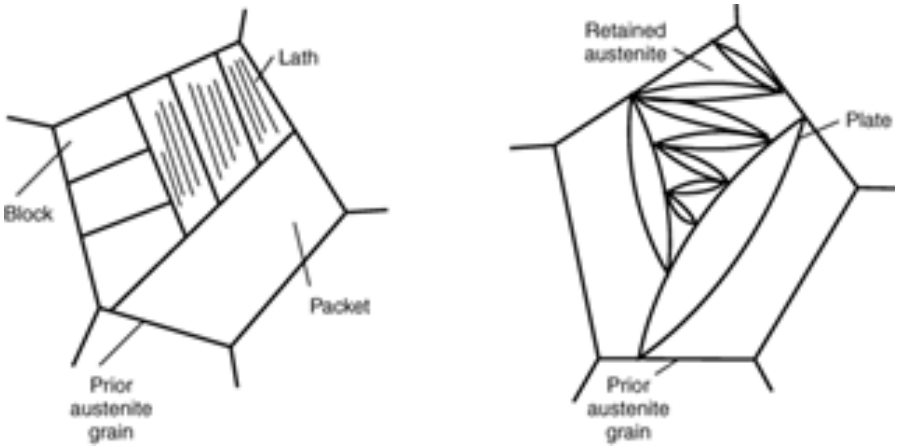

Fig. 1**.** Schematic presentation of (a) Lath Martensite. (b) Plate Martensite [4].

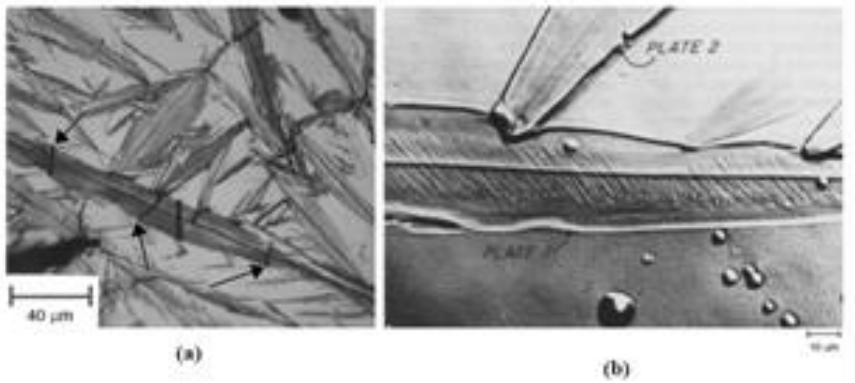

Fig. 2 **(a)** Plate martensite. Arrows indicate microcracks **(b)** Martensite plates. Note the presence of midrib in both plates. Plate 1 shows fine structure consisting of twins [4].

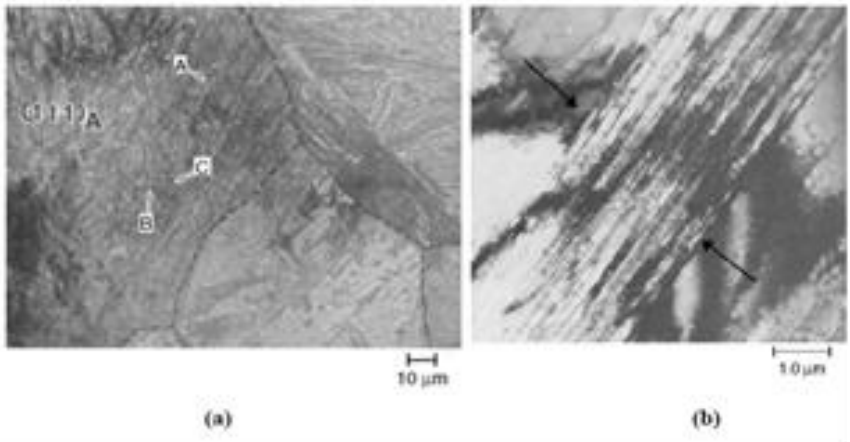

Fig. 3 (a) Optical micrograph showing martensite laths in Fe-0.2%C alloy (b)TEM showing a packet of martensite laths (between arrows) [5,6].

martensite [6]. The martensite start (Ms) temperature generally features on a TTT or CCT diagram as a horizontal line parallel to the time axis. The martensite-start temperature (MS) is the highest temperature at which martensite forms on cooling the parent phase [1,2,4,7]. The, microstructure, (dislocation, vacancies, grain, twins, inter-phase boundaries, and precipitates), external stress and plastic deformation, may sometimes play an important role, but the chemical composition of a steel seems to be a main factor in affecting its Ms [8]. Data related to experimentally determination of martensitic transformation start temperature (Ms temperature) in medium carbon vanadium micro alloyed steel by isothermal treatment seems to be limited. Most of the published results express Ms temperature in terms of the driving force for transformation. Therefore, the purpose of the present study and main goal of the current paper is focused to predict Ms temperature experimentally. Moreover, to clarify the influence addition of the microalloying elements, especially titanium on the martensitic transformation starts forming temperatures in medium carbon vanadium nitrogen micro alloyed steel.

2. EXPERIMENTAL

Two types of vanadium medium carbon micro alloyed forging steels with and without titanium addition have been studied. The chemical compositions of these steel are given in Table 1. The steel was industrially casted by full-scale casting followed by hot forging and hot rolling into 19mm diameter bars. In order to break the dendritic structure, bars were homogenized in laboratory furnace at 1250 °C for 4 hours, in argon as protective atmosphere and subsequently oil quenched. Specimens of 12mm height were cut and austenitized at 1100 °C for 10 min in an argon atmosphere. After austenitization, specimens of both steels were isothermally held at temperatures ranging from (270 °C to 340 °C) for 45s holding times and at 350 °C for 10s holding times then all specimens subsequently water quenched to room temperature. A full description of scheme of isothermal treatments is mentioned in Figure 4. For metallographic inspection, the samples were cut, mechanically ground and then polished to 1µm diamond finish paste using standardized metallographic techniques and subsequently etched in 2 % NITAL for their observation by optical microscopy (OM) and scanning electron microscopy (SEM).

Table 1: Chemical Composition Of The Experimental Steels By (wt%)

Steel Type		Chemical Composition by wt%
V-Ti	V	
0.309	0.256	C
0.485	0.416	Si
1.531	1.451	Mn
0.0077	0.0113	P
0.0101	0.0112	S
0.011	0.002	Ti
0.123	0.099	V
0.0221	0.0235	N

3. Microstructural Characterization

General characteristics of microstructure were observed under optical microscope from samples isothermally treated and polished following standard procedure and etched by 2% NITAL. In order to reveal the fine features in detail, etched samples were also observed by a Field Emission Gun Scanning Microscope (FEGSEM). Elemental analysis in a fine scale was carried out with an Electron Probe Micro-Analysis (EPMA). Camera SX 100 instruments were used for such purpose with an acceleration voltage of 15 kV, beam current 20 mA and with beam diameter of 1 µm.

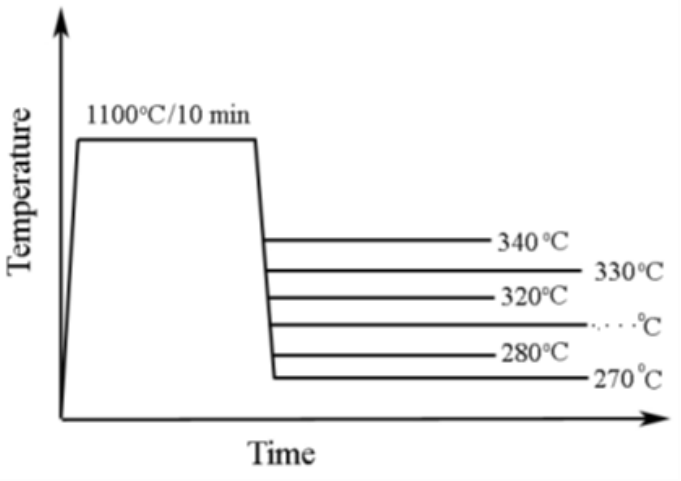

Fig. 4 Schematic presentation of test conditions performed in order to determine Ms temperature.

4. RESULTS AND DISCUSSION

4.1 PAGS Measurement

In the present work, the prior austenite grain boundaries were revealed by using combination of heat treatment and thermal etching [10]. Average austenite grain size was measured using the linear intercept technique that included more than 50 visual fields. As shown in figure 5. The values of average prior austenite grain size experimentally measured are 60 ±5μm for titanium micro alloyed steel and 57 ± 5μm for titanium free micro alloyed steel which is in good agreement with results obtained by similar steels [9].

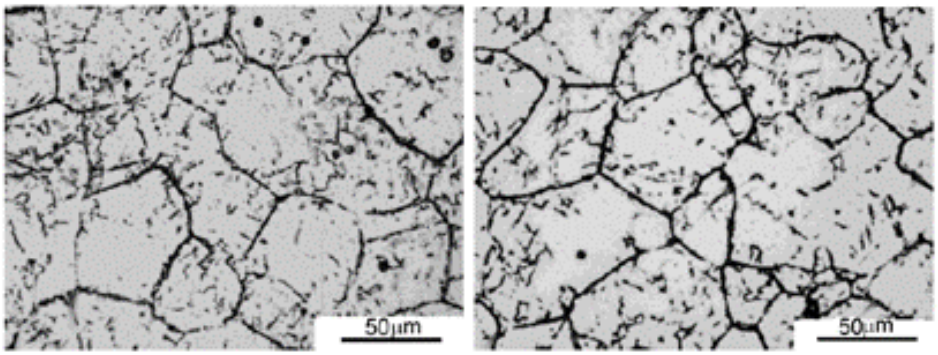

Fig. 5 Optical micrographs showing revealed prior PAGS at 1100 °C (Left Ti and Right Ti free steel).

According to results obtained in this work, (PAGS = 59 ± 6μm) for both steels tested, and compared with information obtained by C. Celada Casero et al [22] as illustrated in Fig. 6, and results obtained by Bhadeshia et al [9], so it is expected for martensite start forming (M_S) temperature to be equal 330 ± 10°C.

4.2 Alloying Elements Distribution

Taking the solubility product of alloying elements into consideration the distribution of vanadium and nitrogen in austenite is rationalized in terms of the temperature for complete dissolution of VN and VC, according to the equation (2.1) and (2.2) in Ref. [11-14], the corresponding results are given in Table 2. It is assumed that the total amount of Ti is within TiN particles, which are insoluble at the reheating temperatures. Using stochiometric ratio Ti:N ═ 3.4 it could be calculated

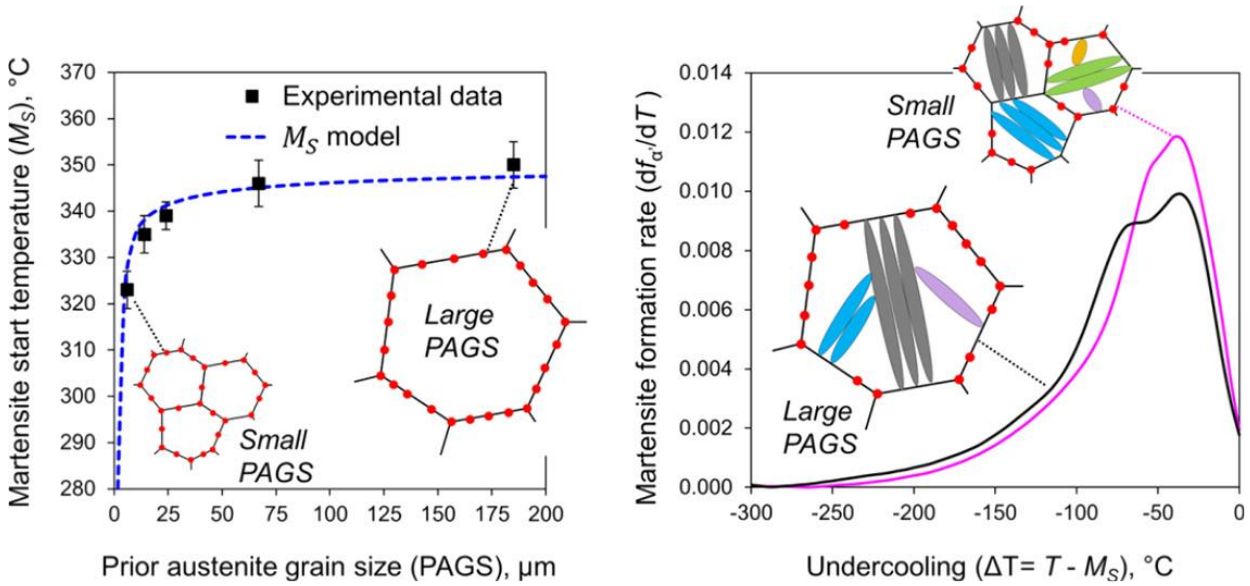

Fig. 6. Evolution of the experimental MS temperatures with PAGS and comparison with the MS model

that titanium ties 6 ppm of nitrogen for Ti free and 32 ppm for Ti steel. Therefore, available amount of nitrogen left in solid solution is slightly reduced in comparison to chemical composition, Table 1.

Table 2. Distribution of alloying elements and temperature for complete dissolution of VN and VC.

Steel	[N](ppm)	[N] Ti (ppm)	[N] Ti free (ppm)	T_{VN}(°C)	T_{VC} (°C)
Ti free	235	229	6	1111	1088
Ti	221	189	32	1114	1084

4.3 Predicting M_S Temperature by Empirical Methods

The martensite–start (M_S) temperature calculated by use of different empirical equations for both steels investigated in present work and the calculation results have shown that, it occurs at temperature 337 ± 20 °C [8,15-20]. It can be estimated by two formulas:

1). The statistical formulas in the general linear form of:

$$Ms = k_0 + \sum k_i w_i$$

$$Ms = 545 - 470.4w_C - 3.96w_{Si} - 37.7w_{Mn} - 21.5w_{Cr} + 38.9w_{Mo}, \quad °C.$$

2). A new empirical model taking into effects of binary interactions. By adding interaction terms into previous equation for C-Si, C-Mn, C-Cr, C-Mo, Si-Mn, Si-Cr, Si-Mo, Mn-Cr, Mn-Mo, and Cr-Mo, a more accurate regressive equation has been obtained [8].

The details of M_S temperature calculated by use of different empirical equation for different authors are given in table 3. Undoubtedly, carbon plays the strongest role in decreasing the Ms. This, is consistent with results shown in Ref. [8,21]. The effect of carbon on martensite morphologies is shown in Fig.7. from which it can be seen that, as the carbon content is lower both M_S and M_f

increase. In regard to the of carbon, as shown in Fig. 8., the martensite morphology exists for a wide range of carbon contents. Most low-carbon steels form lath martensite, while higher-carbon steels form plate martensite and it is possible also to obtain microstructures with a mixture of both plate and lath martensites.

$$\begin{aligned} Ms^{BR} = {} & 540 - 584.9w_C - 23.1w_{Si} - 117.7w_{Mn} - 42.5w_{Cr} \\ & + 49.9w_{Mo} - 62.5w_{C\text{–}Si} + 178.3w_{C\text{–}Mn} \\ & - 10.0w_{C\text{–}Cr} + 52.5w_{C\text{–}Mo} + 117.2w_{Si\text{–}Mn} \\ & + 50.9w_{Si\text{–}Cr} - 142.2w_{Si\text{–}Mo} - 29.2w_{Mn\text{–}Cr} \\ & - 9.7w_{Mn\text{–}Mo} + 69.9w_{Cr\text{–}Mo}, \quad °C \end{aligned} \qquad (5$$

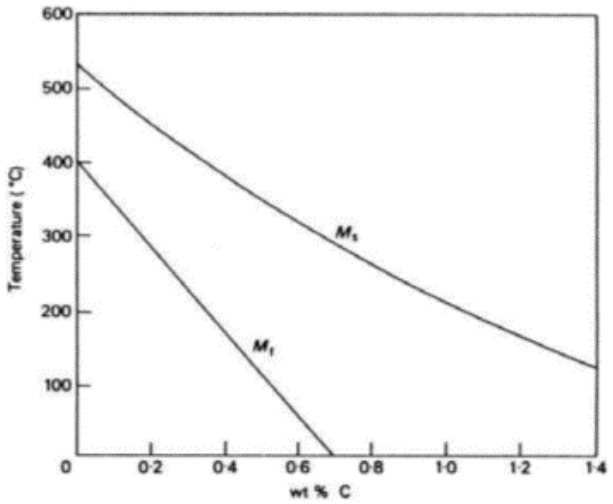

Fig.7. The effect of carbon on Ms and Mf [1]

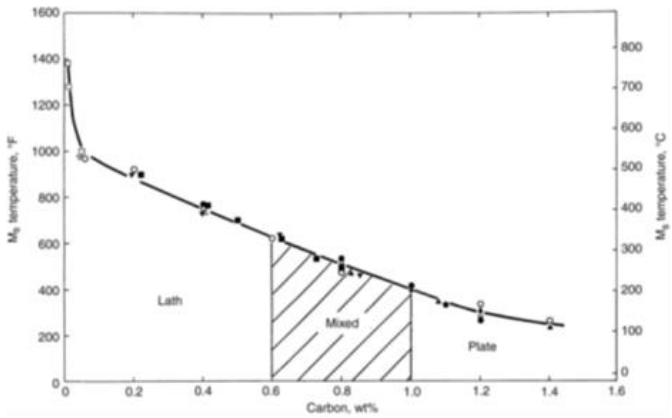

Fig.8. Martensite transformation start temperatures versus carbon content [4].

4.4 M_S Temperature Experimentally Estimated

Start Temperature of the Martensitic Transformation (M_S Temperature) in the present work has been examined by analyzing the result predicted experimentally by use optical microscope (OM) and Field Emission Gun Scanning Microscope (FEGSEM). Moreover, large numbers of experimental data are required and used for complete analysis and predict the Ms temperature. The testing result details are given in table 4., while schedule of testing details is shown in fig.4. The specimens were treated for 45 seconds on each testing temperature, in order to avoid influence of

possible temperature gradient in specimens. The start temperature of the martensitic transformation (Ms Temperature) was experimentally estimated in this work using optical and SEM microscopy and that always exist on TTT diagram by a horizontal line parallel to the time axis (M_S Temperature = 325 ±5 ^oC) in this work is in good agreement with the similar steel given in Ref. [21]. Ms temperature was detected as the highest temperature at which only martensite was present i.e., when no grain boundary ferrites (GBF) were recorded as shown in Fig.9. and Fig. 10. The results empirically or experimentally show that Ti steel has lower Ms Temperature than Ti free steel.

Table 4. M_S Temperature experimentally measured and empirically predicted for Ti and Ti free steels

Ms–Ti Steel [°C]	Ms–Ti free[°C]	Source
336	365	[Eq.4]. [8]
346	373	[Eq.5]. [8]
344	366	[16]
353	377	[17]
335	361	[8]
351	379	[18]
355	381	[19][23]
343	366	[19]
318	359	[20]
320	330	**Experimentally Measured**

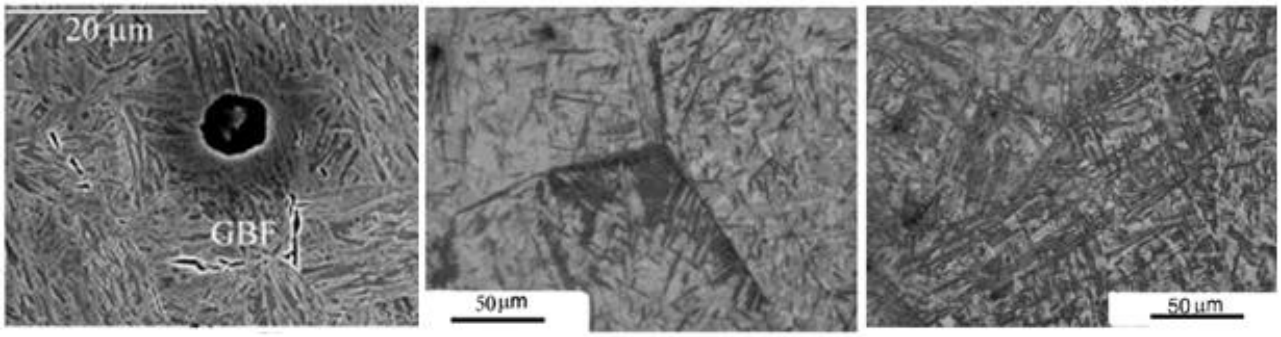

Fig. 9 Typical microstructures showing revealed M_S Temperature, of Ti steel. (Left) SEM image GBF 350 ^oC / 10s (Middle) 330 ^oC / 45s BS at grain boundary triple point. (Right) No any nucleation onset at grain boundary - martensite laths 320 ^oC / 45s.

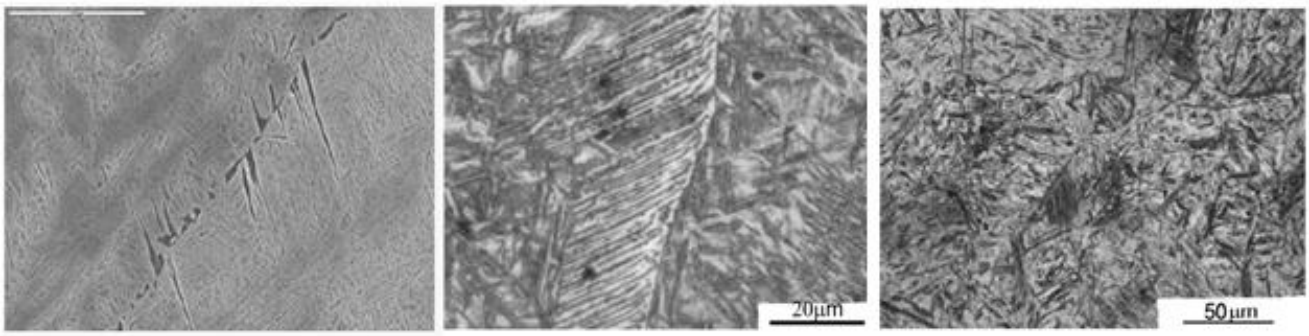

Fig.10 Typical microstructures showing revealed M_S Temperature, of Ti free steel. (Left) SEM image, Grain Boundary Ferrite (GBF) at 350 ^oC / 10 s – bar = 10 µm. (Middle) OM image,340 °C /45s- BS. (Right) 320 °C, no any clear grain boundary nucleation – lath martensite.

5. CONCLUSIOS

In order, to evaluate martensitic transformation start forming temperature at isothermal conditions, series of isothermal tests were performed at (270 - 350 ^oC) for 45 seconds as isothermal holding times. Two vanadium medium carbon micro alloyed steels, V- titanium free (0.256%C,1.451%Mn, 0%Ti) and V- titanium (0.309%C, 1.531%Mn,0.011%Ti), were tested. As conclusion, the martensite–start (M_S) temperature is of vital importance for engineering practice. Therefore, the aim of the current paper was focused to clarify the influence of difference in titanium on martensitic transformation start forming temperature. Start temperature of the martensitic transformation (M_S temperature) in this work was experimentally estimated using optical microscopy (OM) and field emission gun scanning electron microscopy (FEGSEM). The (M_S) temperature was detected as the highest temperature at which only martensite was present i.e when no grain boundary ferrites (GBF) were recorded. The experimentally predicted results showing that titanium steel has lower Ms temperature, which is in good agreement with results empirically predicted using different empirical equation (Table 4) and also in complete agreement with similar steel given in Ref. [21]. Moreover, regarding to the lack of significant variation in the (M_S) temperature values obtained in this study. These is attributed to two reasons. In titanium steel, (1) the higher content of carbon and Mn (table 1) enhancing the formation of martensite i.e. decreases the (M_S) temperature. (2) the higher content of vanadium and addition of (0.011%Ti) as microalloying element, who is very well known for its hardenability effects i.e. increases the (M_S) temperature. In summary, the addition of titanium to vanadium micro alloyed steel in this work seems to be balanced by a slightly higher C and Mn content leading to limited effect on nucleation stage of austenite decomposition.

REFERENCES

[1] H.K.D.H. Bhadeshia, Bainite in Steels, Second Edition, The Institute of Metals, London, UK (2006).
[2] Steels Microstructure and Properties, H.K. Bhadeshia, R.W Honeycombe, Elsevier Ltd, London, (2006).
[3] A. R. Marder, Structure-Property Relationships in Ferrous Transformation Products, Phase Transformation of Ferrous Alloys, Proc. Int. Conf., TMS (1984)11–41.
[4] Martensitic Structures, Metallography and Microstructures, ASM Handbook 9, ASM International, (2004)165–178.
[5] G. B. Olson, W. S. Owen, Ed., Martensit*e:* A Tribute to Morris Cohen, ASM International, (1992).
[6] G. Krauss, Martensite in Steel: Strength and Structure, Mater. Sci. Eng. A 273–275, (1999) 40–57.
[7] M. Cohen, G. B. Olson, P. C. Clapp, Proc. Int. Conf. on Martensitic Trans. ICOMAT, Massachusetts (1979) 1.
[8] J. Wang, P. van der Wolk, S. van der Zwaag. Mater. Trans, JIM,41(2000)761-768.
[9] Hong-Seok Yang, H.K.D.H. Bhadeshia, Scripta Materialia 60 (2009) 493–495.
[10] C. Garcia de Andres, F.G. Caballero, C. Capdevila, D. San Martin, Mater. Charact. 49 (2003) 121–127.
[11] D. Glisic, N. Radovic, A. Koprivica, A. Fadel and D. Drobnjak: ISIJ Int., 50 (4) (2010) 601–606.
[12] H. Adrian, Proc. of Int. Conf. Microalloying ’95, ISS, Warrendale, PA, USA, (1995) 285.
[13] W. Roberts, A. Sandberg, Report IM-1489, Swedish Institute for Metals Research (1980).
[14] Dj. Drobnjak, A. Koprivica, Microalloyed Bar and Forging Steels, Edited by C.J. Van, Tyne, G. Krauss, D.K. Matlock, The Minerals, Metals &Materials Society, (1996) 93-107.
[15] Steel Forming and Heat Treating, Handbook, Antonio Augusto Gorni São Vicente. (2011) 24.
[16] A.E. Nehrenberg: Transactions of the AIME, 167, 1946, 494.in ref. [15].

[17] K.W. Andrews, Empirical formulae for the calculation of some transformation temperatures, Journal of the Iron and Steel Institute 7(1965) 721-727.
[18] B. Mintz, The influence of aluminium on the strength and impact properties of steel, Int. Con. on TRIP-aided H. S. Ferrous Alloys, Ghent (2002) 379-382.
[19] S. Chupatanakul, P. Nash, D. Chen, Met. and Mat. Int., 12 (2006)453~458.
[20] M. Arjomandi, H. Khorsand, S. H. Sadati, H. Addoos, Defect and Diffusion Forum 273-276 (2008) 329-334.
[21] G. F. Caballero, M. J. Santofimia, C. Garcı´a-Mateo, C. G. de Andre´s Mat. Trans, 45 (2004) 3272 – 3281.
[22] C. Celada-Casero, J. Sietsma, M. J. Santofimia, Materials and Design 167 (2019) 107625.
[23] A.Grajcar, H. Krzton, J.of Achievements in Mat. And Manuf. Eng., 35/2 (2009) 169-176.